LETTERS

Increased seasonality through the Eocene to Oligocene transition in northern high latitudes

James S. Eldrett[1], David R. Greenwood[2], Ian C. Harding[3] & Matthew Huber[4]

A profound global climate shift took place at the Eocene–Oligocene transition (~33.5 million years ago) when Cretaceous/early Palaeogene greenhouse conditions gave way to icehouse conditions[1–3]. During this interval, changes in the Earth's orbit and a long-term drop in atmospheric carbon dioxide concentrations[4–6] resulted in both the growth of Antarctic ice sheets to approximately their modern size[2,3] and the appearance of Northern Hemisphere glacial ice[7,8]. However, palaeoclimatic studies of this interval are contradictory: although some analyses indicate no major climatic changes[9,10], others imply cooler temperatures[11], increased seasonality[12,13] and/or aridity[12–15]. Climatic conditions in high northern latitudes over this interval are particularly poorly known. Here we present northern high-latitude terrestrial climate estimates for the Eocene to Oligocene interval, based on bioclimatic analysis of terrestrially derived spore and pollen assemblages preserved in marine sediments from the Norwegian–Greenland Sea. Our data indicate a cooling of ~5 °C in cold-month (winter) mean temperatures to 0–2 °C, and a concomitant increased seasonality before the Oi-1 glaciation event. These data indicate that a cooling component is indeed incorporated in the $\delta^{18}O$ isotope shift across the Eocene–Oligocene transition. However, the relatively warm summer temperatures at that time mean that continental ice on East Greenland was probably restricted to alpine outlet glaciers.

A rapid two-step shift in benthic foraminiferal $\delta^{18}O$ (Oi-1 glaciation)[1,2] marks a period of dramatic global change, with the development of an Antarctic ice sheet by the Eocene–Oligocene transition, ~33.5 million years (Myr) ago. The proposed driving mechanism for this climate change is the lowering of atmospheric CO_2 from high levels during the Eocene epoch (>1,000 parts per million by volume, p.p.m.v.) to lower levels (~560 p.p.m.v.) in the Oligocene epoch[4–6]. However, it has been argued that the changes in $\delta^{18}O$ composition across this boundary are too large to be explained by ice build-up on Antarctica alone[2], which, combined with continued debate over whether there was ocean cooling associated with the $\delta^{18}O$ shift[3,15–17], raises the possibility of contemporaneous ice development in the Northern Hemisphere. Although recent sedimentological evidence supports the development of some continental ice in the Northern Hemisphere at that time[7,8,18], proxy-based CO_2 estimates suggest that atmospheric CO_2 concentrations were still at least twice the pre-industrial level during the Eocene–Oligocene transition[4,5], which is above the modelled critical threshold for Northern Hemisphere ice development[6,19].

Despite these estimates, there is ample evidence to suggest climate cooling in the late Eocene to Oligocene[11,20,21]. However, there are substantial differences in the extent and timing of the presumed cooling, some records demonstrating little evidence for temperature change[9,10], while other low-resolution records indicate increased seasonality in the Oligocene, shown by a fall in cold-month mean temperatures (CMMTs)[12] and increased aridity[9,10,15,21]. These continental records are mostly from high altitude or mid- to high latitudes, but whereas there is some information on high southern latitude Eocene–Oligocene conditions[22], no comparable information is available for high northern latitudes to enable accurate global climate reconstruction. Moreover, in these high-latitude sequences there is little or no calcareous content, owing to carbonate dissolution, negating the use of foraminiferal $\delta^{18}O$ and Mg/Ca temperature proxies.

Therefore, we examined the acid-insoluble organic fraction of the sediments from three key Ocean Drilling Program sites (ODP sites 643, 985 and 913; Supplementary Fig. S1), producing the first high-resolution terrestrial climate reconstructions using plant palynomorphs (spore and pollen assemblages). In addition, because of limited climate proxy records previously available at these latitudes, we compared our terrestrial climate record with modelling simulations of the mid-Eocene (partial pressure of CO_2, p_{CO_2} = 1,120 p.p.m.v.) and the early Oligocene (p_{CO_2} = 560 p.p.m.v.).

We constructed a composite section spanning the Eocene to Oligocene by calibrating dinocyst events to the geomagnetic polarity timescale[23], enabling the first palaeoclimatic reconstruction of Greenland through the Eocene and early Oligocene. ODP site 913 (75° 29.356' N, 6° 56.810' E, present water depth ~3,300 m) is the most complete high northern latitude Eocene to Oligocene succession[23]. Spore and pollen assemblages from ODP site 913 are abundant throughout the Eocene sequence (Fig. 1), but the Oligocene is characterized by reworking and reduced recovery (see Supplementary Information). Therefore, this site is supplemented by ODP site 643 (67° 47.11' N, 01° 02.0' E), with a preserved Eocene–Oligocene boundary interval and by ODP site 985 (66° 56.49' N, 6° 27.01' W) with a complete lower Oligocene section (Fig. 2). Despite their different core locations, new modelling data supports the contention that East Greenland is the likely vegetation source area for all sites during the Eocene and Oligocene, allowing climate reconstruction of the Greenland landmass (see Supplementary Information).

The lower Eocene palynofloral assemblage at Site 913B is comprised of taxa typical of extant lowland freshwater swamps on the United States southeast coastal plain[24], namely Taxodiaceae–Cupressaceae (*Taxodium* or *Metasequoia* type), several types of ferns (for example, *Lygodium* and other Schizeaceae), palms/cycads (Arecaceae or Cycadales), *Carya* (Juglandaceae), *Nyssa* (Nyssaceae), and *Salix* (Salicaceae) grains (Fig. 1). The occurrence of palms/cycads in these sediments indicates mesothermal to megathermal conditions and CMMTs over 5 °C (refs 24, 25).

The palynofloral assemblage recovered from middle to upper Eocene sediments from ODP site 913 are consistent with other records for that time[25,26], with characteristic microthermal to mesothermal Pinaceae pollen (for example, *Abies, Picea, Pinus* and

[1]Shell Exploration and Production UK Ltd, 1 Altens Farm Road, Nigg, Aberdeen, AB12 3FY, UK. [2]Biology Department, Brandon University, 270 18th Street, Brandon, Manitoba, R7A 6A9, Canada. [3]School of Ocean and Earth Science, National Oceanography Centre, University of Southampton, European Way, Southampton, SO14 3ZH, UK. [4]Earth and Atmospheric Sciences Department, Purdue Climate Change Research Center, Purdue University, 550 Stadium Mall Drive, West Lafayette, Indiana 47906, USA.

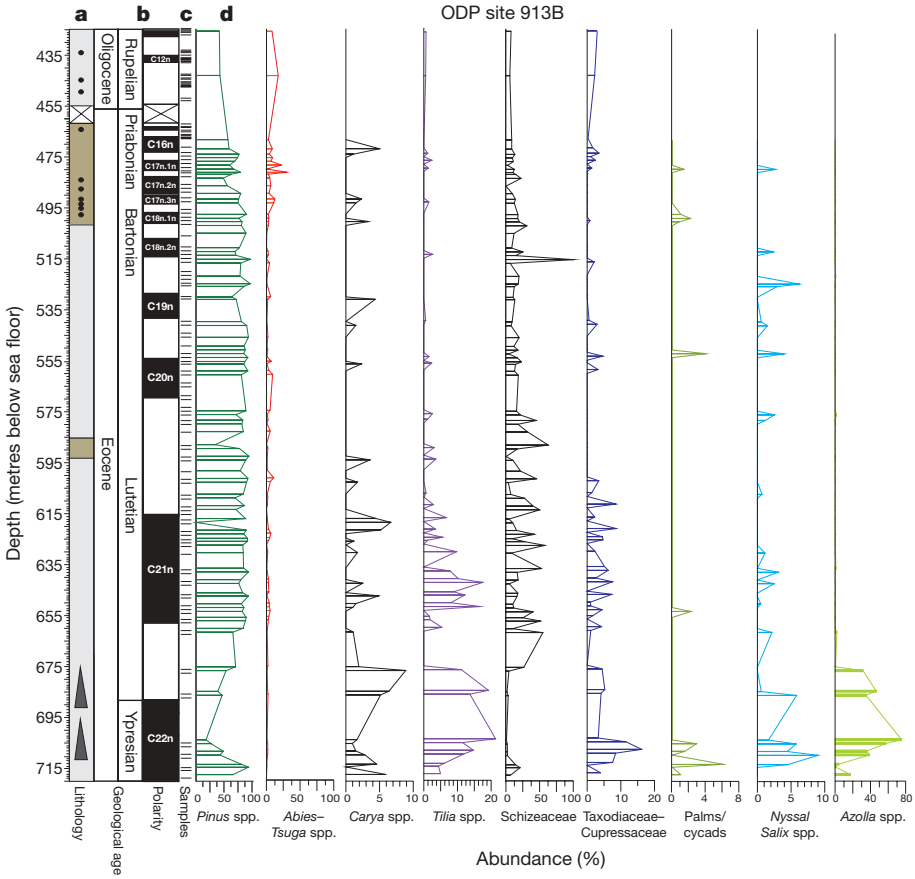

Figure 1 | Data from ODP site 913. **a**, Lithology of the core, comprising biosiliceous clay (brown), clay and silty clay (light grey), macroscopic dropstones (solid circles), and fining upward sequences (triangles). **b**, Age model. The chronology of ODP site 913 is based on direct correlation with the geomagnetic polarity timescale reported in ref. 23. **c**, Samples analysed for palynology. **d**, Selected pollen and spore percentage abundance.

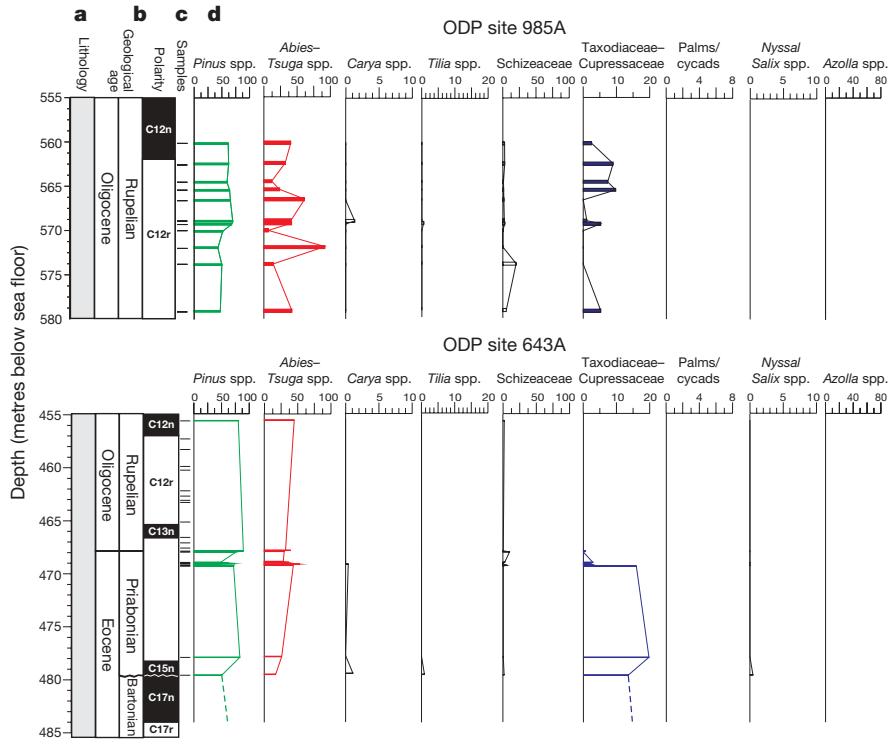

Figure 2 | Data from ODP sites 985 and 643. **a**, Lithology of the core, comprising clay and silty clay (light grey). **b**, Age models: the chronology for ODP sites 985 and 643 is based on direct correlation to the geomagnetic polarity timescale reported in ref. 23. The chronology for the basal Oligocene for ODP sites 985 and 643 are presented in the Supplementary Information. **c**, Samples analysed for palynology. **d**, Selected pollen and spore percentage abundance.

the rare *Tsuga*) being dominant, indicating extensive coniferous forests on Greenland. Mesothermal conifers such as Taxodiaceae–Cupressaceae and *Sciadopitys*, and dicotyledons such as *Carya*, *Juglans* and *Tilia* are still represented, indicating both allochthonous long-distance pollen transport of preferred wind-dispersed pollen (for example, Pinaceae) from cooler—perhaps mountainous—regions of East Greenland to the marine sediments at Site 913B, combined with shorter-distance transport from the warmer lowland conditions prevailing at the coast. Our climate model indicates that wind speed and direction would not have been sensitive to likely climate changes during the Eocene–Oligocene transition, so we interpret trends in the palynological record (below) as representing changes in the climatic conditions in the source regions and not as changes in atmospheric circulation (Supplementary Information).

Uppermost Eocene–lower Oligocene sediments from the two more southerly ODP sites 643A and 985A (Fig. 1) yield palynofloral assemblages dominated by Pinaceae (*Abies, Picea* and *Pinus*), but with a substantial increase in *Tsuga* and *Abies* relative to the mid-Eocene assemblages of Site 913B (Fig. 2). Moreover, the absence of mesothermal frost-sensitive taxa (that is, palms/cycads, *Engelhardtia* and *Nyssa*) and rarity of other mesothermal elements (such as 'Taxodiaceae', *Tilia*, *Carya*), suggests the widespread development of an evergreen *Pinus*-, *Tsuga*- and *Abies*-dominated conifer forest under microthermal conditions by the Oligocene. The shifts in dominance and floral composition documented in the latest Eocene to earliest Oligocene by the pollen sums, although partly confounded by their different core locations (see Supplementary Information), appears to show a displacement of warmer, moderately diverse mixed conifer–broadleaf vegetation and plant types from lowland sites caused by the expansion of a cooler, less-diverse Pinaceae-dominated coniferous forest type.

To derive a quantified palaeoclimatic signal from the pollen and spore assemblages we have applied bioclimatic analysis using the nearest living relatives (NLRs) method[24] (see Supplementary Information) to reconstruct mean annual temperature, mean annual precipitation, CMMT and warm month mean temperature (WMMT) for the Eocene to Oligocene transition (Fig. 3). Our data indicate that the Eocene Greenland climate was generally warm, with mean annual temperature 14 °C ± 3 °C, CMMT > 5 °C and WMMT ≈ 18–24 °C, respectively (Fig. 3b–d). A small number of samples in the late Eocene from Site 913B give estimates of CMMT of 4–5 °C and WMMT < 20 °C. We calculated the first precipitation estimates for the Eocene of Greenland, which are high (mean annual precipitation >120 cm yr^{-1}), although there are large uncertainties in this estimate (Fig. 3e). The mean annual temperature estimates generated are consistent with previous estimates of mid-Eocene climate records from Axel Heiberg Island in the Canadian Arctic further to the west[25]. However, our mid-Eocene CMMT estimates are slightly warmer (>5 °C) than that estimated using leaf physiognomy from macrofloras from Axel Heiberg Island (~0 °C, ref. 25). Cooler winter conditions in the Eocene Canadian Arctic than in Greenland are supported by our model simulations (Fig. 4), but may also reflect the different methodologies used, because leaf physiognomy has been shown to yield cooler estimates than NLR-based approaches for the same fossil assemblage[24,25].

The latest Eocene to early Oligocene climate estimates from ODP sites 643 and 985 have been corrected for palaeolatitude (0.4 °C per 1° latitude, as presented in ref. 25; see Supplementary Information) so that they can be directly compared with ODP site 913. Our data indicates that for the latest Eocene to Oligocene, mean annual temperature is estimated at 10–11 °C ± 3 °C, representing a decline of ~3 °C ± 3 °C from the mid- to late Eocene interval. However,

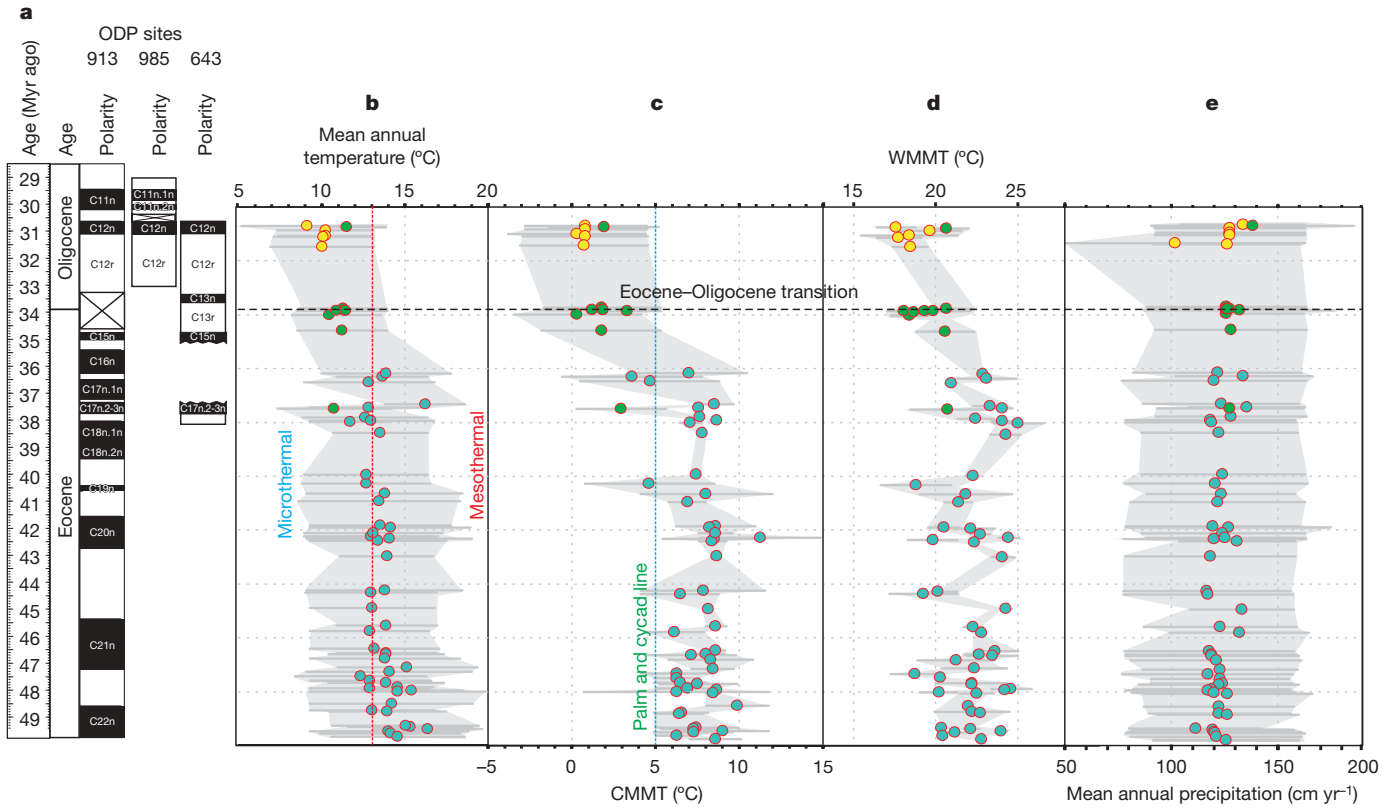

Figure 3 | Data from ODP sites 913, 643 and 985, Norwegian–Greenland Sea. **a**, Composite chronologies based on direct correlation to the geomagnetic polarity timescale (ref. 23; see Supplementary Information). **b**–**e**, Composite record of Eocene to Oligocene climate data. **b**, Mean annual temperature. Red dashed line defines transition from mesothermal to microthermal conditions. **c**, CMMT. Blue dashed line represents the temperature at which palms/cycads do not occur, as discussed in ref. 25. **d**, WMMT. **e**, Mean annual precipitation. For all plots, blue circles indicate ODP site 913, yellow circles indicate site 985 and green circles indicate site 643. **b**–**e**, Horizontal error bars and shaded area represent the minimum and maximum estimate returned from the method (ref. 24).

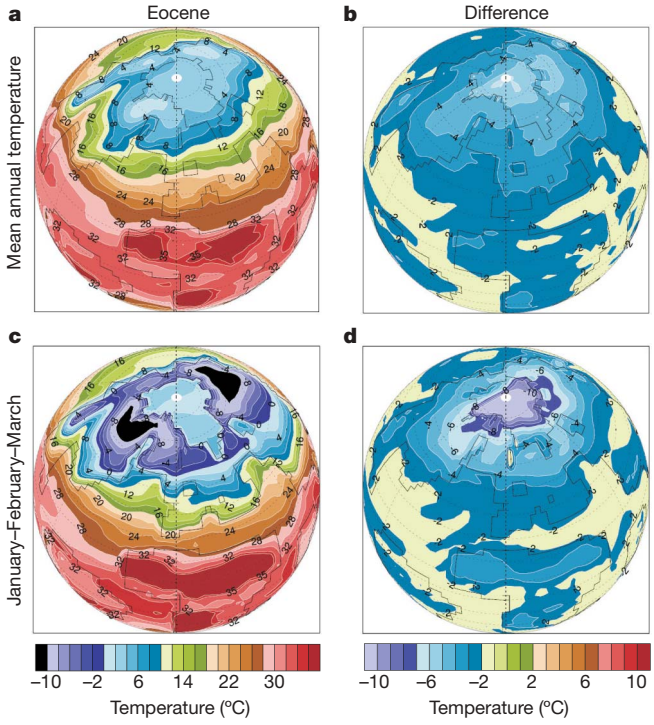

Figure 4 | Model surface temperature results (shown in °C) supporting bioclimatic estimates. Left panels show Eocene (p_{CO_2} = 1,120 p.p.m.v.) temperatures. Right panels show temperature differentials between the Eocene and the Oligocene (p_{CO_2} = 1,120–560 p.p.m.v.). **a**, **b**, Mean annual temperature; **c**, **d**, January–February–March (representative of CMMT).

although this amount of cooling is consistent with earlier records[27] and our global circulation model simulations (Fig. 4a, b), it is also within the error limits of the data. Our data also indicates a slight decline in WMMT, although this may not be significant because our estimates fall within the error limits and range seen in the Eocene. Nor do we see a significant change in mean annual precipitation (>120 cm yr^{-1}), suggesting continued high precipitation and relatively warm summer temperatures during the earliest Oligocene. There is some indication of cyclical variability in the WMMT mid-Eocene record. However, of greatest significance, winter temperatures (as CMMT) show greater variability than in the mid-Eocene, leading up to the Eocene–Oligocene boundary interval with some estimates of CMMT ~5 °C, and consistently cooler values in the early Oligocene (CMMT ~0–2 °C) than recorded for most of the mid- to late Eocene record (CMMT ~8 °C). The drop in CMMT in the latest Eocene to Oligocene is apparent even without the latitudinal correction.

Our interpretation of cooler winters in the latest Eocene to early Oligocene on Greenland is consistent with other climate records[10,12], while our global circulation model simulations (Fig. 4c, d), indicate that our climate record for Greenland is representative of the northern high latitudes as a whole. Therefore our data indicates that in high northern latitudes the Eocene–Oligocene transition saw a shift towards more extreme seasonal temperature ranges, greater in magnitude than the mean annual temperature changes. The shift to cooler winters is reflected in particular by (1) a loss or dramatic reductions of both freezing-intolerant palms/cycads (plants that today are not found in climates where CMMT < 5 °C, ref. 25) and warm-temperate broadleaf taxa such as hickory (*Carya*), *Engelhardtia*, tupelo (*Nyssa*) and basswood (*Tilia*) by the late Eocene, and (2) by a rise to dominance in the latest Eocene and Oligocene of typical mid-latitude to boreal forest conifers such as fir (*Abies*), hemlock (*Tsuga*) and other Pinaceae. The change in vegetation we report occurs before the Oi-1 glaciation event, and is contemporaneous with the first ice build-up on Greenland ~38 Myr ago[7]. Our climate model results are consistent with this pattern, clearly showing the initiation of thick, extensive winter sea-ice and thin perennial Arctic sea-ice across the transition interval and a concomitant decrease of winter temperatures of greater magnitude than that in mean annual temperature. Other grain size evidence from ODP site 913 for an earlier inception of ice on Greenland (44 Myr ago, ref. 28) is discounted here, because these deeper sediments contain no macroclasts/dropstones and are characterized by abundant concretions, authigenic quartz grains and possible contourite deposits, all of which point towards a non-glacial origin for these deeper grain-size records.

The climatic estimates presented here provide the first continental temperature constraints for high northern latitudes for the Eocene to Oligocene, and therefore have implications for the ongoing debate concerning Cenozoic ice budgets, the timing of the inception of Northern Hemisphere glaciation[1–3,7,8,16–18,29,30], and our understanding of Cenozoic atmospheric carbon dioxide levels[4–6,19]. The cooler CMMTs and increased seasonality we document occurs before the Cenozoic uplift in Greenland commencing ~36 Myr ago[31], but the contemporary northward movement of Greenland to impinge on the Eurasian basin and the Lomonosov ridge[32] may have influenced Northern Hemisphere ice build-up in the earliest Oligocene, especially at high altitudes. However, the relatively warm summer temperatures at that time means it is likely that Northern Hemisphere ice on East Greenland was restricted to alpine outlet glaciers[3,7,30]. This interpretation is consistent with high-resolution Eocene isotope records[30] and both proxy and model reconstructions of Cenozoic CO_2 (refs 4, 5), which remain well above the critical threshold (~2.8 times the pre-industrial level) for bipolar ice-sheet development[6,19]. The winter temperature decrease is consistent with the initiation of thick, extensive Arctic Ocean winter sea-ice occurring at $p_{CO_2} \approx$ 560 p.p.m.v. The winter cooling revealed by the data may have increased deep convection and been responsible for the apparent initiation of Northern Component Water formation during this interval[33].

METHODS SUMMARY

Palynology. The palynological techniques used to process the 141 samples are described in ref. 23. Residues were analysed using a stereo-binocular microscope until the entire slide was counted for terrestrial palynomorphs.

Bioclimatic analyses. The method of bioclimatic analysis is essentially the same as described in ref. 24, but with additional data sources enabling more robust and diverse climatic profiles to be developed for each taxon, as described in the online-only Methods. To account for the low species richness found in many samples, we tested the effect of rarefaction of individual species-rich samples on the estimate by recalculating the estimate using successively fewer of the available NLRs with climate profiles. Rarefied samples with fewer than 12 NLRs with climate profiles produced widely divergent estimates at the same species richness, whereas the estimates for rarefied samples with 12 or more NLRs were consistently well within the error of the estimate (see Supplementary Information). Accordingly, only samples with 12 or more NLRs with climate profiles were used in our analysis. Those taxa that were used in this study and their NLRs can be found in Supplementary Table S1.

Climate model simulations. To estimate wind and current directions and provide a physical framework for understanding the climate signal recorded by proxies, we conducted a series of palaeoclimate general circulation model experiments. We used the atmospheric component (CAM version 3) of the National Center for Atmospheric Research, Community Climate System Model (version 3), at a spectral resolution of T42. The sea surface temperatures used to drive these simulations were derived from long, equilibrated, fully coupled, synchronous, unaccelerated simulations of the Eocene (p_{CO_2} = 1,120 p.p.m.v.) and Oligocene (p_{CO_2} = 560 p.p.m.v.). Topography, bathymetry and vegetation distributions and other boundary conditions are appropriate for this time interval and they and the model are described in depth in the online-only Methods.

Full Methods and any associated references are available in the online version of the paper at www.nature.com/nature.

Received 23 October 2008; accepted 9 April 2009.

1. Zachos, J. C., Pagani, M., Sloan, L., Thomas, E. & Billups, K. Trends, rhythms, and aberrations in global climate 65 Ma to present. *Science* **292**, 686–693 (2001).
2. Coxall, H. K., Wilson, P. A., Pälike, H., Lear, C. H. & Backman, J. Rapid stepwise onset of Antarctic glaciation and deeper calcite compensation in the Pacific Ocean. *Nature* **433**, 53–57 (2005).

3. Lear, C. *et al.* Cooling and ice growth across the Eocene-Oligocene transition. *Geology* **36** (3) 251–354, doi:210.1130/G1124 (2008).
4. Pagani, M. *et al.* Marked decline in atmospheric carbon dioxide concentrations during the Paleogene. *Science* **309,** 600–603 (2005).
5. Pearson, P. N. & Palmer, M. R. Atmospheric carbon dioxide over the past 60 million years. *Nature* **406,** 695–699 (2000).
6. DeConto, R. M. & Pollard, D. Rapid Cenozoic glaciation of Antarctica induced by declining atmospheric CO_2. *Nature* **421,** 245–249 (2003).
7. Eldrett, J., Harding, I. C., Wilson, P., Butler, E. & Roberts, A. Continental ice in Greenland during the Eocene and Oligocene. *Nature* **446,** 176–179 (2007).
8. Moran, K. *et al.* The Cenozoic palaeoenvironment of the Arctic Ocean. *Nature* **441,** 601–605 (2006).
9. Kohn, M. J. *et al.* Climate stability across the Eocene-Oligocene transition, southern Argentina. *Geology* **32,** 621–624 (2004).
10. Grimes, S. T., Hooker, J. J., Collinson, M. E. & Mattey, D. P. Summer temperatures of late Eocene to early Oligocene freshwaters. *Geology* **33,** 189–192 (2005).
11. Zanazzi, A., Kohn, M. J., MacFadden, B. J. & Terry, D. O. Large temperature drop across the Eocene–Oligocene transition in central North America. *Nature* **445,** 639–642 (2007).
12. Ivany, L. C., Patterson, W. P. & Lohmann, K. C. Cooler winters as a possible cause of mass extinctions at the Eocene/Oligocene boundary. *Nature* **407,** 887–890 (2000).
13. Terry, D. O. Jr. Paleopedology of the Chadron Formation of northwestern Nebraska; implications for paleoclimatic change in the North American Midcontinent across the Eocene-Oligocene boundary. *Palaeogeogr. Palaeoclimatol. Palaeoecol.* **168,** 1–38 (2001).
14. Sheldon, N. D., Retallack, G. J. & Tanaka, S. Geochemical climofunctions from North American soils and application to paleosols across the Eocene-Oligocene boundary in Oregon. *J. Geol.* **110,** 687–696 (2002).
15. Dupont-Nivet, G. *et al.* Tibetan Plateau aridification linked to global cooling at the Eocene–Oligocene transition. *Nature* **445,** 635–638 (2007).
16. Lear, C. H., Rosenthal, Y., Coxall, H. K. & Wilson, P. A. Late Eocene to early Miocene ice-sheet dynamics and the global carbon cycle. *Paleoceanography* **19,** PA4015, doi:10.1029/2004PA001039 (2004).
17. Lear, C. H., Elderfield, H. & Wilson, P. A. Cenozoic deep-sea temperatures and global ice volumes from Mg/Ca in benthic foraminiferal calcite. *Science* **287,** 269–272 (2000).
18. St John, K. Cenozoic ice-rafting history of the Central Arctic Ocean: terrigenous sands on the Lomonosov ridge. *Paleoceanography* **23,** PA1S05 (2008).
19. DeConto, R. *et al.* Thresholds for Cenozoic bipolar glaciation. *Nature* **455,** 652–656 (2008).
20. Kobashi, T., Grossman, E. L., Yancey, T. E. & Dockery, D. T. III. Reevaluation of conflicting Eocene tropical temperature estimates; molluskan oxygen isotope evidence for warm low latitudes. *Geology* **29,** 983–986 (2001).
21. Retallack, G. J. *et al.* Eocene-Oligocene extinction and paleoclimatic change near Eugene, Oregon. *Geol. Soc. Am. Bull.* **116,** 817–839 (2004).
22. Thorn, V. C. & DeConto, R. M. Antarctic climate at the Eocene/Oligocene boundary; climate model sensitivity to high latitude vegetation type and comparisons with the palaeobotanical record. *Palaeogeogr. Palaeoclimatol. Palaeoecol.* **231,** 134–157 (2006).
23. Eldrett, J. S., Harding, I. C., Firth, J. V. & Roberts, A. P. Magnetostratigraphic calibration of Eocene-Oligocene dinoflagellate cyst biostratigraphy from the Norwegian-Greenland Sea. *Mar. Geol.* **204,** 91–127 (2004).
24. Greenwood, D. R., Archibald, S. B., Mathewes, R. W. & Moss, P. T. Fossil biotas from the Okanagan Highlands, southern British Columbia and northeastern Washington State: climates and ecosystems across an Eocene landscape. *Can. J. Earth Sci.* **42,** 167–185 (2005).
25. Greenwood, D. R. & Wing, S. L. Eocene continental climates and latitudinal temperature-gradients. *Geology* **23,** 1044–1048 (1995).
26. Norris, G. Spore-pollen evidence for early Oligocene high-latitude cool climatic episode in northern Canada. *Nature* **297,** 387–389 (1982).
27. Schouten, S. *et al.* Onset of long-term cooling of Greenland near the Eocene-Oligocene boundary as revealed by branched tetraether lipids. *Geology* **36,** 147–150, doi:10.1130/G24332A.1 (2008).
28. Tripati, A. *et al.* Evidence for Northern Hemisphere glaciation back to 44 Ma from ice-rafted debris in the Greenland Sea. *Earth Planet. Sci. Lett.* **265,** 112–122 (2008).
29. Billups, K. & Schrag, D. P. Application of benthic foraminiferal Mg/Ca ratios to questions of Cenozoic climate change. *Earth Planet. Sci. Lett.* **209,** 181–195, doi:10.1016/S0012–821X(03)00067–0 (2003).
30. Edgar, K. M., Wilson, P. A., Sexton, P. F. & Suganuma, Y. No extreme bipolar glaciation during the main Eocene calcite compensation shift. *Nature* **448,** 908–911 (2007).
31. Bonow, J. M., Japsen, P., Lidmar-Bergstrom, K., Chalmers, J. A. & Pedersen, A. K. Cenozoic uplift of Nuussuaq and Disko, West Greenland—elevated erosion surfaces as uplift markers of a passive margin. *Geomorphology* **80,** 325–337 (2006).
32. Brozena, J. M. *et al.* New aerogeophysical study of the Eurasia Basin and Lomonosov Ridge: implications for basin development. *Geology* **31,** 825–828 (2003).
33. Via, R. K. & Thomas, D. J. Evolution of Atlantic thermohaline circulation: Early Oligocene onset of deep-water production in the North Atlantic. *Geology* **34,** 441–444 (2006).

Supplementary Information is linked to the online version of the paper at www.nature.com/nature.

Acknowledgements This research used samples provided by the Ocean Drilling Program (ODP). ODP was sponsored by the US National Science Foundation (NSF) and participating countries under management of Consortium for Ocean Leadership. D.R.G.'s research is supported by NSERC (Canada). We thank S. Akbari for sample preparation.

Author Contributions J.S.E. and I.C.H. conceived the project, collected samples and data, and completed the palynological interpretation. D.R.G. and J.S.E. completed the bioclimatic analysis of the spore–pollen record, and led the write-up. M.H. conducted all numerical climate modelling and Lagrangian trajectory analysis. All authors were involved in developing the palaeoclimate interpretation in this work

Author Information Reprints and permissions information is available at www.nature.com/reprints. Correspondence and requests for materials should be addressed to J.S.E. (james.eldrett@shell.com).

METHODS

Bioclimatic analyses. The method of bioclimatic analysis is essentially the same as the coexistence approach of ref. 34, and requires the development of 'climatic profiles' for living taxa, based on the climatic envelopes controlling the distributions of modern plant genera. A library of climatic profiles is then produced for individual taxa, based on climatic values such as mean annual temperature, mean annual precipitation, and CMMT[35,36]. The climatic profiles used in this study were from four sources: (1) a study of North American tree genera[36], (2) the Palaeoflora database[37] (and personal communication T. Utescher, Bonn Univ.), which includes a wider range of extant plant genera than the North American database and also includes European and Asian distribution records (for example, *Engelhardtia*, *Pterocarya*), (3) Natural Resources Canada[38], used for North American herbaceous and shrub taxa not present in the other databases (for example, *Lonicera*) and (4) the Australian National Herbarium database[39], which was analysed using the ANUCLIM software[35], and used for tropical and temperate taxa not represented in the other databases (for example, *Gleichenia*). Where values were available for the same taxon from more than one source, sources (1) and (2) were used preferentially, or the values with the widest range were used (for example, coolest minimum and warmest maximum for CMMT).

Climate model simulations. The NCAR Community Climate System Model version 3 (CCSM3)[40] is a coupled climate model with separate components that can be integrated separately or in tandem for the atmosphere (CAM), land surface/vegetation (CLM), sea ice (CSIM), and ocean (POP). For the purposes of this study relatively high atmospheric resolution was considered beneficial (because the relevant Arctic land-sea distributions are not well resolved at T31, a typical palaeoclimate general circulation model resolution) so we performed stand-alone atmospheric general circulation model simulations using CAM3 (ref. 41) at T42 resolution driven by sea surface temperatures derived from Eocene–Oligocene fully coupled CCSM3 simulations. The coupled simulations were carried out at the standard palaeoclimate resolution parameters for CCSM3, with T31 resolution in the atmospheric model (CAM3), and a nominal resolution of $\times 3'$ in the ocean[42,43]. These fully coupled simulations were carried out for over 1,500 years and are fully equilibrated at a range of CO_2 values as described in ref. 44. The global mean sensitivity of the model is about 2.2 °C per doubling, both for these simulations and for modern to doubled CO_2 concentrations. This is the normal range of sensitivity for the CCSM3 model[45]. The two CAM3 stand-alone atmospheric general circulation model simulations used in this study are performed with p_{CO_2} values of 1,120 and 560 p.p.m.v. and driven by sea surface temperatures and sea-ice fractions from the coupled simulations with the same CO_2. All other parameters were held constant. In all cases, vegetation, orography and topography, and other parameters were based on reconstructed Eocene distributions[46–48].

Accordingly, to estimate palaeo-wind transports, and surface temperatures we used the T42 CAM3 simulations. The simulations are fully equilibrated: the top-of-atmosphere radiative imbalance is $-0.047\ W\ m^{-2}$ and $-0.004\ W\ m^{-2}$ for the simulated low and high p_{CO_2} concentrations respectively; global mean terrestrial temperatures reached quasi-steady state after 5 years and the simulations were continued for at least an additional 60 years. Means from the last 15 years are discussed. All differences discussed are statistically significant at the 95% level based on a Student's *t*-test.

To determine the vegetation source region and the influence of atmospheric transportation of spore–pollen transport pathways we performed a fully Lagrangian tracer investigation for this region. Lagrangian back-trajectories (refs 49, 50) were calculated centred on the Greenland Sea and followed back for ten days using the six-hourly low-level wind fields. The trajectories were started every ten days and for each year, and this was repeated for ten years to produce a meaningful ensemble of back-trajectories (that is, approximately 360 separate releases of a puff of passive tracer particles). The ensemble mean distribution should be considered as an approximate probability distribution function for the likelihood that any given region is a potential source is shown in Supplementary Figs S4–S6.

34. Utescher, T., Mosbrugger, V. & Ashraf, A. R. Terrestrial climate evolution in northwest Germany over the last 25 million years. *Palaios* **15,** 430–449 (2000).
35. Greenwood, D. R., Archibald, S. B., Mathewes, R. W. & Moss, P. T. Fossil biotas from the Okanagan Highlands, southern British Columbia and northeastern Washington State: climates and ecosystems across an Eocene landscape. *Can. J. Earth Sci.* **42,** 167–185 (2005).
36. Thompson, R. S., Anderson, K. H. & Bartlein, P. J. Atlas of relations between climatic parameters and distributions of important trees and shrubs in North America. *US Geol. Surv. Prof. Pap.* 1650, A & B (USGS, 1999).
37. Palaeoflora Database at ⟨http://www.geologie.uni-bonn.de/Palaeoflora/Palaeoflora_home.htm⟩.
38. Natural Resources Canada at ⟨http://planthardiness.gc.ca/ph_main.pl?lang=en⟩.
39. Integrated. Botanical Information System (IBIS) Australian National Herbarium at ⟨http://www.anbg.gov.au/cgi-bin/anhsir⟩.
40. Collins, W. D. *et al.* The Community Climate System Model Version 3 (CCSM3). *J. Clim.* **19,** 2122–2143 (2006).
41. Collins, W. D. *et al.* The formulation and atmospheric simulation of the Community Atmosphere Model version 3 (CAM3). *J. Clim.* **19,** 2144–2161 (2006b).
42. Yeager, S., Shields, C., Large, W. & Hack, J. J. The low resolution CCSM3. *J. Clim.* **19,** 2545–2566 (2006).
43. Kiehl, J. T. & Shields, C. A. Climate simulation of the latest Permian: implications for mass extinction. *Geology* **33,** 757–760 (2005).
44. Liu, Z. *et al.* Global cooling during the Eocene-Oligocene climate transition. *Science* **323,** 1187–1190 (2009).
45. Kiehl, J. T., Shields, C. A., Hack, J. J. & Collins, W. D. The climate sensitivity of the Community Climate System Model Version 3 (CCSM3). *J. Clim.* **19,** 2584–2596 (2006).
46. Sewall, J. O., Sloan, L. C., Huber, M. & Wing, S. Climate sensitivity to changes in land surface characteristics. *Glob. Planet. Change* **26,** 445–465 (2000).
47. Huber, M. & Sloan, L. C. Heat transport, deep waters, and thermal gradients: Coupled simulation of an Eocene ''greenhouse'' climate. *Geophys. Res. Lett.* **28,** 3481–3484 (2001).
48. Huber, M., Sloan, L. C. & Shellito, C. in *Causes and Consequences of Globally Warm Climates in the Early Paleogene* (eds Wing, S. L., Gingerich, P. D., Schmitz, B. & Thomas, E.) *Geol. Soc. Am. Spec. Pap.* **369,** 25–47 (2003).
49. Yang, H. & Pierrehumbert, R. T. Production of dry air by isentropic mixing. *J. Atmos. Sci.* **51,** 3437–3454 (1994).
50. Huber, M., McWilliams, J. C. & Ghil, M. A climatology of turbulent dispersion in the troposphere. *J. Atmos. Sci.* **58,** 2377–2394 (2001).